Electronic supplementary information

Fast oxygen exchange kinetics of pore-free $Bi_{1-x}Sr_xFeO_{3-\delta}$ thin films

Anja Wedig, Rotraut Merkle, Benjamin Stuhlhofer,

Hanns-Ulrich Habermeier, Joachim Maier and Eugene Heifets

Max Planck Institute for Solid State Research, Stuttgart, Germany

Sample preparation

Stoichiometric amounts of Bi_2O_3, $SrCO_3$ and Fe_2O_3 were ground together in a mortar, dried for 2 h at 770°C and subsequently ball-milled for 1 h. The resulting mixture was calcined twice at 1050°C ($Bi_{0.5}Sr_{0.5}FeO_{3-\delta}$) or 1100°C ($Bi_{0.2}Sr_{0.8}FeO_{3-\delta}$) for 8 h with intermediate ball milling for 1 h. X-ray diffraction (XRD) confirmed the formation of a single phase cubic perovskite structure. For the preparation of targets for pulsed laser deposition (PLD), the obtained powder was pressed into cylindrical pellets with about 1 cm in diameter and the pellets sintered in air for 8 h at 1100°C. The density after sintering was estimated to about 85% of the theoretical density which was considered sufficient for PLD targets. Pellets with a higher density for electrical conductivity and thermal expansion measurements were produced by spark plasma sintering (SPS) (HP D 5, FCT Systeme, Germany) in graphite dies. Cylindrical pellets with approx. 5 mm in diameter were sintered at 800°C for 5 min under a pressure of 350 MPa. After additional heat treatment in air at 1050°C ($Bi_{0.5}Sr_{0.5}FeO_{3-\delta}$) or 1100°C ($Bi_{0.2}Sr_{0.8}FeO_{3-\delta}$) for 12 h in a conventional furnace, the pellet density reached 96% ($Bi_{0.5}Sr_{0.5}FeO_{3-\delta}$) and about 90% ($Bi_{0.2}Sr_{0.8}FeO_{3-\delta}$) respectively of the theoretical value.

Thin films were deposited by PLD on polished 9.5 mol% Y_2O_3-doped ZrO_2 (YSZ) single crystals with (100) orientation and dimensions $5 \times 5 \times 0.5$ mm^3 (CrysTec, Germany). The deposition was performed by means of a KrF excimer laser (LPX 200, Lambda Physik, Germany) with a wavelength of 248 nm at a repetition frequency of 5 Hz and an energy density per pulse of 1.6 J/cm^2. The substrate was kept at a temperature of 650°C during the ablation process, and the oxygen pressure was adjusted to 0.4 mbar. After the deposition, the films with a thickness of 150 nm were annealed at 650°C for 10 min to 20 min in 1 bar oxygen.

Bulk sample characterization

Thermogravimetric analyses were performed on a STA 449 C Jupiter thermobalance (Netzsch, Germany) in different N_2/O_2 mixtures at a total gas flow rate of 50 ml/min. To remove possible impurities such as water or carbonate, the powder was first heated to 850°C and equilibrated for 1 h. Then, the sample was cooled down to 300°C with cooling rates of 3 K/min (from 850°C to 600°C), 1.5 K/min (from 600°C to 450°C) and 0.7 K/min (from 450°C to 300°C). The same procedure was repeated in the opposite direction to check whether full equilibration had been reached at any temperature. Since for $Bi_{0.2}Sr_{0.8}FeO_{3-\delta}$ the equilibration showed hysteresis at low temperatures, the heating/cooling rates were decreased for this composition to 1 K/min (from 850°C to 600°C), 0.5 K/min (from 600°C to 450°C) and 0.2 K/min (from 450°C to 300°C). To properly arrange the curves obtained for the individual oxygen partial pressures with respect to each other, the mass change upon stepwise changing the oxygen partial pressure was detected at 700°C. Buoyancy effects were eliminated by subtracting the mass changes measured with an empty alumina crucible (quartz glass was found to undergo a reaction with the sample material under the applied conditions).

For cerimetric titrations, about 100 ml of 6 mol/l HCl solution, previously flushed with N_2, were transferred into a Schlenk flask containing approx. 100 mg of the sample powder and about 100 mg of $FeCl_2{\cdot}4H_2O$ (Acros Organics, Belgium) under a flux of N_2 and the flask sealed immediately. After letting the mixture react for about 30 min with ultrasonic stirring, the titration was performed under a N_2 flux with 0.05 mol/l $Ce(SO_4)_2$ solution (Riedel-de Haën, Germany) and 1/40 mol/l 1,10-phenanthroline iron(II) sulfate (ferroin) solution (Merck, Germany) as indicator until the solution changed its colour from orange to green. The $Ce(SO_4)_2$ solution was standardized using $FeC_2H_4(NH_3)_2(SO_4)_2{\cdot}4H_2O$ (Alfa Aesar, Germany) and the purity of the $FeCl_2{\cdot}4H_2O$ confirmed via a blind titration. To check the validity of the method, $SrFeO_{3-\delta}$ with $\delta \approx 0$ prepared by high oxygen pressure treatment[1] was used as analyte. The reproducibility of δ determined from three titrations for each sample was ±0.001. The systematic error of the method was estimated not to exceed 0.01.

To measure the electrical conductivity, an approx. 200 nm thick layer of Pt was sputtered using an Auto 306 sputtering system (Edwards, UK) on both faces of the pellets received from SPS and subsequent annealing (see above). Electrodes cut out from Pt foil were mechanically pressed on top of the sputtered layers. These electrodes were contacted by two Pt wires each to conduct simplified four probe measurements. This setup was chosen since the geometry of the sample did not allow for a real four probe arrangement. The measured sample resistance might therefore also contain contributions from the electrode-sample contact resistance, but the latter is assumed to be negligible. The sample was placed in a quartz tube flushed with 50 ml/min of N_2/O_2 mixtures to provide the required oxygen partial pressure. An AC voltage with an amplitude of 10 mV was applied to record impedance spectra. The intercept with the real axis was interpreted as the sample (plus contact) resistance and used to calculate the electrical conductivity.

For thermochemical expansion measurements, bars with approx. $3.5 \times 3.5 \times 1.5$ mm^3 in size were cut from the pellets produced by SPS and subsequent annealing (see above). The bars were placed in a dilatometer (DIL802, Bähr, Germany) flushed with 50 ml/min of appropriate mixtures of O_2 and inert gas. After heating the samples to 800°C to remove water/carbonate and equilibration for 30 min, they were cooled to room temperature with 1 K/min, kept at this temperature for 1 h and again heated to 800°C with 1 K/min to verify the reproducibility of the measured length changes. The mean coefficient of linear thermochemical expansion $\overline{\mathrm{TEC}}$ was calculated to $(1/L_0)(\Delta L/\Delta T)$ (L_0: initial length of the specimen at temperature T_0, T_0: reference temperature 20°C, $\Delta L = L_\mathrm{i} - L_0$, $\Delta T = T_\mathrm{i} - T_0$) in the present study. For the thermochemical expansion coefficients from literature depicted in Table 1 of the main article, the exact definitions are not known. From the magnitude however we conclude that they represent rather mean than instantaneous coefficients of linear thermochemical expansion, the latter being defined as $(1/L_0)(\mathrm{d}L/\mathrm{d}T)$. Thermochemical expansion measurements were carried out at $p(O_2) = 10^{-3}$ bar and $p(O_2) = 1$ bar. All measurements were corrected against the thermochemical expansion detected for a sapphire standard sample with similar dimensions.

Thin film characterization

X-ray diffractograms were recorded by a Philips PW 3710 X-ray diffractometer using Cu K_α radiation. Scanning electron microscopy (SEM) was performed on a Merlin (Zeiss, Germany, Fig. S2a and Fig. S2c) and an EsB CrossBeam 1540 instrument (Zeiss, Germany, Fig. S2b and Fig. S2d). For analysis of the film cross-sectional area, a lamella was cut out by a gallium ion beam at an acceleration voltage of 30 kV after local deposition of a Pt layer to reduce electrostatical charging. Energy-dispersive X-ray (EDX) analyses conducted on a Stereoscan 420 scanning electron microscope (Leica, Germany) confirmed the compositional homogeneity of the thin films. Inductively coupled plasma optical emission spectroscopy (ICP-OES) was carried out on a Ciros CCD spectrometer (Spectro, Germany) after dissolution of film samples with a nominal thickness of 450 nm in a 2:3 mixture of concentrated hydrochloric acid and concentrated nitric acid.

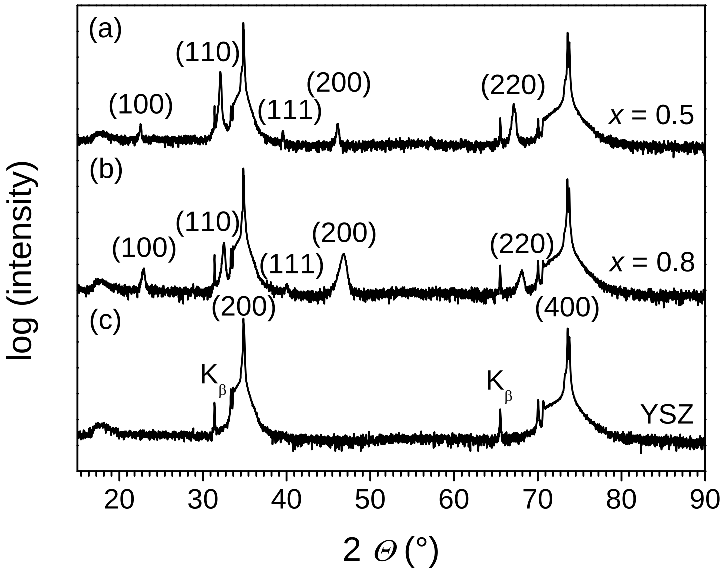

Fig. S1 X-ray diffractograms of 150 nm thick Bi$_{1-x}$Sr$_x$FeO$_{3-\delta}$ films with x = (a) 0.5 and (b) 0.8 deposited by PLD on YSZ (100) single crystals. The diffractogram of (c) a bare YSZ substrate is shown for comparison.

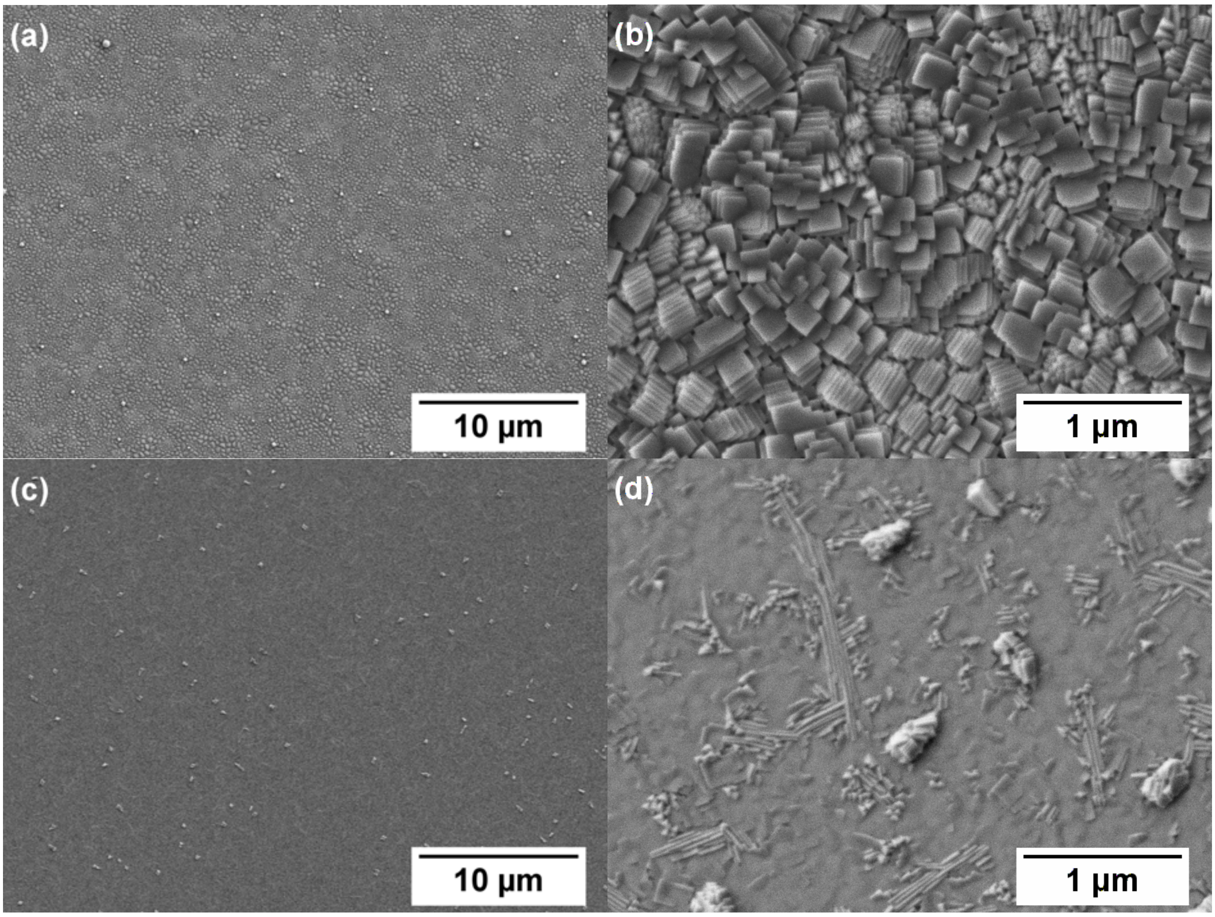

Fig. S2 SEM images of 150 nm thick Bi$_{1-x}$Sr$_x$FeO$_{3-\delta}$ films with x = (a), (b) 0.5 and (c), (d) 0.8 deposited by PLD on YSZ (100) single crystals. The films appear smooth when reproduced with low resolution but reveal a pronounced texture at higher resolution (especially for x = 0.5); nevertheless, the increase in surface area due to surface roughening is considered negligible compared to the increase in surface area caused by the deliberate porosity of the conventional screen-printed electrodes.

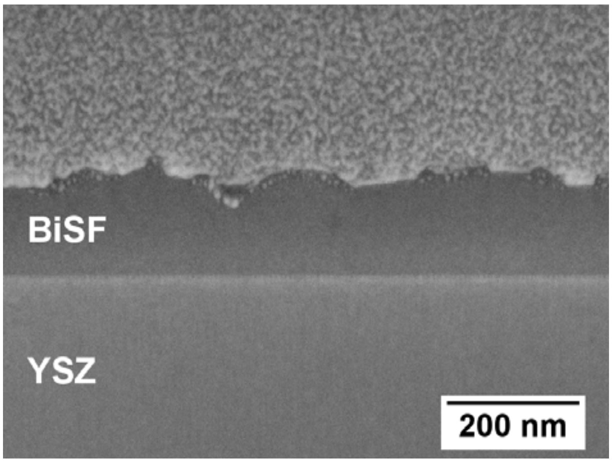

Fig. S3 SEM image of a cross section of a $Bi_{0.5}Sr_{0.5}FeO_{3-\delta}$ (BiSF) thin film grown by PLD on a YSZ (100) single crystal. A Pt layer was deposited onto the film surface prior to measurement in order to reduce electrostatical charging. No pores are visible penetrating deeper into the film.

Electrochemical impedance measurements on microelectrode samples were performed following a standard procedure to account for any degradation of the oxygen incorporation rate with time observed for related perovskite-type mixed-conducting oxides.[2,3] First, absolute R_s values were measured on 10 different microelectrodes on the same YSZ substrate with 60 µm in diameter at 750°C and $p(O_2)$ = 0.2 bar. Directly afterwards, temperature-dependent measurements were conducted on another 60 µm electrode. The temperature was decreased in steps of 25°C from 750°C to the temperature where recording of an evaluable spectrum was still possible within the applied frequency range (typically around 550°C). Then, the same procedure was repeated in the opposite direction with the temperature increasing in steps of 50°C. The activation energy derived from this second measurement series was found to be by 0.1 eV on average smaller than the one from the first series corresponding to an increase in R_s by about 21% from the initial to the final measurement at 750°C. Therefore, degradation effects can be considered negligible within the time span required to measure the temperature dependence. Next, $p(O_2)$-dependent measurements were carried out on another microelectrode with 60 µm in diameter increasing the $p(O_2)$ from initially 10^{-4} bar to about 1 bar by one order of magnitude in each step. A final measurement at a $p(O_2)$ of approx. 10^{-2} bar was used to estimate the degradation of the sample and yielded an R_s higher by about 23% than the first measurement at the same $p(O_2)$. The exponent n calculated from the last three measurements (at $p(O_2) = 10^{-1}$ bar, 1 bar and 10^{-2} bar) was by 0.03 on average higher than n determined from all measurements except the last one (at $p(O_2) = 10^{-2}$ bar). Thus, it can be assumed that n is underestimated by roughly 0.03/2 probably due to degradation effects. In the described way, two microelectrode samples resulting from a single PLD run were measured for each of the two compositions. Each single data point from microelectrode measurements depicted in Fig. 3 therefore represents the average of the values obtained from two different samples.

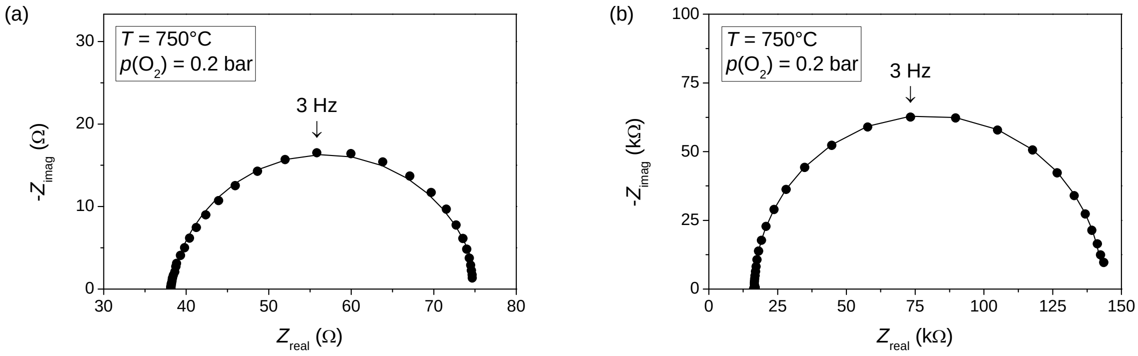

Fig. S4 Impedance spectra of pore-free 150 nm thin $Bi_{0.2}Sr_{0.8}FeO_{3-\delta}$ films measured on (a) a macroscopic sample (YSZ single crystal coated on both sides) and (b) a microelectrode with 60 µm diameter on a YSZ single crystal.

For macroscopic samples, a similar routine was applied. Macroscopic samples were placed in a small quartz tube flushed with the desired gas mixture, whereas the complete setup for microelectrode measurements was accommodated in a comparatively big vacuum chamber where equilibration of the gas atmosphere proceeded rather slowly. As a consequence, one day was sufficient to complete a measurement series on a macroscopic sample, whereas microelectrode measurements could only be accomplished within two days (with intermediate cooling of the sample prior to measuring the $p(O_2)$ dependence). Therefore, degradation effects can be expected to have less influence on the macroscopic samples. This might also be an explanation for the lower absolute values of the surface resistance observed in $p(O_2)$-dependent measurements on macroscopic samples (Fig. 3b). For technical reasons, only results from a single temperature and $p(O_2)$ series for each composition are shown in Fig. 3. Absolute values (Table 1) were however calculated using values from two macroscopic samples of each composition.

The evaluation of macroscopic and microelectrode impedance spectra was based on the equivalent circuit shown in Fig. S5. In addition to the electrolyte resistance, the high-frequency axis intercept R_b might also contain contributions from electrical sheet resistance within the electrode film as well as contact resistance between the probe needle and the electrode. The low ionic conductivity of YSZ calculated from R_b of both macroscopic and microelectrode impedance spectra and the observed decrease in R_b from $Bi_{0.5}Sr_{0.5}FeO_{3-\delta}$ to $Bi_{0.2}Sr_{0.8}FeO_{3-\delta}$, *i.e.* with increasing electrical conductivity of the electrode material, indeed indicate a noticeable influence of sheet resistance and/or contact resistance on the high-frequency axis intercept.

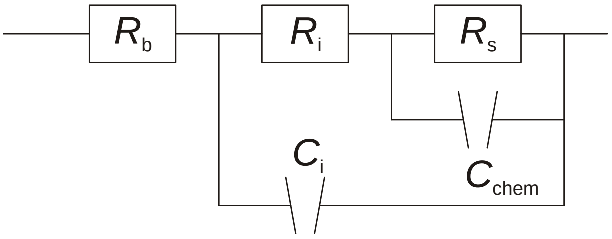

Fig. S5 Equivalent circuit used for the evaluation of electrochemical impedance spectra.[4] R_b: electrolyte resistance, R_i: interfacial resistance, R_s: surface resistance, C_i: interfacial capacitance, C_{chem}: chemical capacitance.

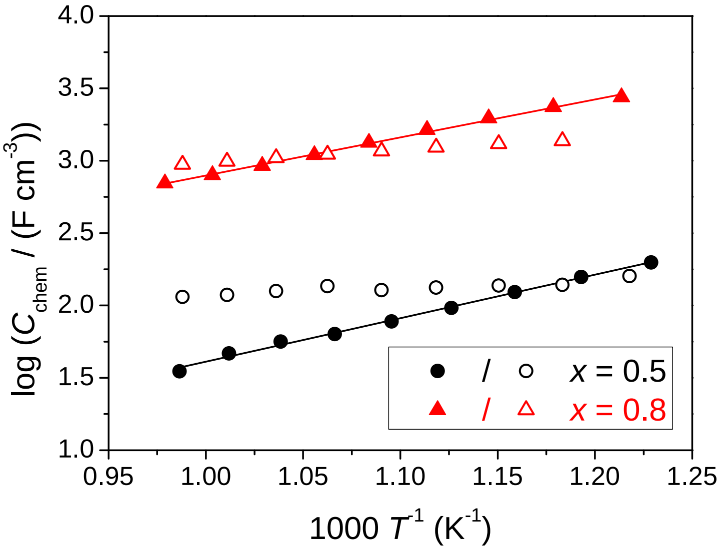

Fig. S6 Temperature dependence of the chemical capacitance C_{chem} of $Bi_{1-x}Sr_xFeO_{3-\delta}$ with $x = 0.5$ and 0.8 at $p(O_2) = 0.2$ bar obtained from impedance spectra. Solid symbols: macroscopic samples, open symbols: microelectrode samples. The $p(O_2)$ dependence of C_{chem} obeys $C_{chem} \propto (p(O_2))^{-n}$ with average n values of 0.17 for $x = 0.5$ and 0.09 for $x = 0.8$.

---

[1] M. Vračar, A. Kuzmin, R. Merkle, J. Purans, E. A. Kotomin, J. Maier and O. Mathon, *Phys. Rev. B*, 2007, **76**, 174107.
[2] F. S. Baumann, J. Fleig, M. Konuma, U. Starke, H.-U. Habermeier and J. Maier, *J. Electrochem. Soc.*, 2005, **152**, A2074.
[3] L. Wang, R. Merkle and J. Maier, *J. Electrochem. Soc.*, 2010, **157**, B1802.
[4] F. S. Baumann, J. Fleig, H.-U. Habermeier and J. Maier, *Solid State Ionics*, 2006, **177**, 1071.